Tetrahedron: *Asymmetry* 21 (2010) 177–186

Contents lists available at ScienceDirect

Tetrahedron: *Asymmetry*

journal homepage: www.elsevier.com/locate/tetasy

Limitations, mechanism and understanding of the origins of stereocontrol in (*S*)-dimethylsulfonium-(*p*-tolylsulfinyl)methylide-mediated epoxidation reactions

Wanda H. Midura *, Marek Cypryk

Centre of Molecular and Macromolecular Studies, Polish Academy of Sciences, 90-363 Lodz Sienkiewicza 112, Poland

ARTICLE INFO

Article history:
Received 16 November 2009
Accepted 21 January 2010

ABSTRACT

The reaction of the (*S*)-dimethylsulfonium-(*p*-tolylsulfinyl)methylide with aldehydes gave α,β-epoxy sulfoxides with high enantioselectivity and diastereoselectivity dependent on the aldehyde. The mechanism of the 'model' reactions [ylide substituted with Me S(O) or Ph S(O) with MeCHO or PhCHO] has been studied in detail using density functional theory.

1. Introduction

Enantiopure sulfoxides have become an important class of chiral auxiliaries due to their ease of preparation, synthetic versatility and straightforward removal.[1] The sulfinyl group acts as an electron-withdrawing group and activates carbon–carbon double bonds for conjugate addition and stabilizes the corresponding α-carbanion. To date, a large number of asymmetric syntheses using chiral sulfoxides[2] have been investigated in a wide range of reactions such as the reduction of β-ketosulfoxides,[3] the Michael addition of nucleophiles to the activated α,β-unsaturated sulfoxides,[4] the Diels–Alder reaction of vinyl sulfoxides[3] and C–C bond formation using sulfoxide-stabilized carbanions.[5] The reaction of α-sulfinyl carbanions with aldehydes and ketones, leading to β-hydroxyalkyl sulfoxides, is generally known to be highly diastereoselective with respect to the α-sulfinyl carbon, but poorly diastereofacially selective with respect to attack on the carbonyl component. While simple optically active sulfoxides, such as methyl *p*-tolyl sulfoxide, give products with poor diastereoselectivity, those containing another functional group such as an ester, sulfide or amide, which exert a chelating effect in the transition state, led to the formation of optically active α-sulfinyl esters, sulfides or amides, which are very useful reagents in asymmetric aldol-type condensations. When a halogen substituent is introduced to a sulfoxide moiety as a good leaving group, ring closure can be accomplished to give an epoxide.

There are two main ways of preparing an epoxide enantioselectively: by enantioselective oxidation of the prochiral double bond[6,7] and by enantioselective alkylidenation of carbonyls using either a carbene or Darzens type reagent.[8,9] In addition to α-chlorosulfoxides, sulfonium ylides can be used for this purpose. Generally, all the asymmetric conversions of aldehydes into oxiranes are mediated by sulfur ylides, in which chirality is located in the sulfonium moiety.[10]

2. Results

Continuing our work on the utilization of optically active sulfinyl compounds in asymmetric synthesis,[11] we designed a new type of chiral sulfur ylide, containing an enantiopure sulfinyl group bonded to the ylidic carbon atom.[12] The sulfonium salt required for the generation of the title ylide **1a** was obtained by methylation of (−)-(*S*)-*p*-tolyl methylthiomethyl sulfoxide with methyl iodide in the presence of equimolar amount of silver tetrafluoroborate in dry ethyl ether, followed by addition of acetone/water 1:1 mixture, filtration of the precipitated AgI and evaporation of the solvents. The crystalline salt (**2**) formed in quantitative yield was fully characterized. The starting optically active thioacetal monosulfoxide was prepared by treatment of optically active (+)-(*S*)-bromomethyl *p*-tolyl sulfoxide with sodium methanethiolate[13] or preferably by the substitution of (−)-menthyl (−)-(*S*)-*p*-toluenesulfinate by methylthiomethyl-lithium as described by Gennari.[14] Treatment of the sulfonium salt **2** with sodium hydride in DMSO solution at room temperature afforded dimethylsulfonium *p*-tolylsulfinylmethylide **1a** in quantitative yield, as evidenced by ^{1}H NMR.[12] Dimethylsulfonium *p*-tolylsulfinylmethylide **1a** was also prepared by deprotonation with sodium hydride in another polar solvent MeCN to provide homogeneity of the reaction and also under heterogenous conditions: in THF solution using BuLi as a base. Later on, we determined that the ylide is generated in situ when the reaction of sulfonium salt **2** with the electrophile is performed in CH_2Cl_2 solution in the presence of potassium carbonate or potassium hydroxide.

To demonstrate the utility of the sulfinylmethylide **1a** in asymmetric synthesis we first applied it to the conversion of aldehydes

* Corresponding author. Tel.: +48 42 6803202; fax: +48 42 6847126.
E-mail address: whmidura@cbmm.lodz.pl (W.H. Midura).

0957-4166/$ - see front matter © 2010 Elsevier Ltd. All rights reserved.
doi:10.1016/j.tetasy.2010.01.012

to epoxides. In the first attempt, the ylide **1a** generated in DMSO solution at room temperature was in situ treated with benzaldehyde affording 3-phenyl-2-(*p*-tolylsulfinyl)-oxirane **4a** as a mixture of two diastereomers in a 1.5:1 ratio. This promising result prompted us to check all the other conditions that the ylide could be generated and their influence on the stereochemical results. In order to determine the scope and limitation of the epoxidation we performed the reaction with different types of aldehydes. The results are shown in Table 1.

Table 1 reveals that the results of epoxidation depends on the aldehyde used as well as on the base and the solvent. The ratio of *trans* versus *cis* diastereomers formed was about 1 to 1, when alkyl aldehydes were used, but for aryl aldehydes it was slightly different and varied from 1.5:1 to 8:1. This was probably caused by the bulkiness of the aryl group, since the best results were observed for 1-naphthaldehyde. A lower *trans/cis* selectivity was observed when the reaction was carried out in DMSO but was slightly higher in an acetonitrile solution, as well in a non-polar solvent (CH_2Cl_2). At this point it is necessary to underline the very high facial stereoselectivity observed during the addition of the ylide **1a** to the carbonyl group for all the reactions examined. The third diastereomer ($2R,3R,S_S$) was formed in very small amount (2–8.5%) and under some reaction conditions this product was not even detected. The fourth possible diastereomer was not observed. This means that the stereochemistry on the ylidic carbon (C-2 in oxirane) is completely controlled by the chirality of the sulfinyl center.[15]

What could be the explanation of this high stereoselectivity? The major problem for an acyclic auxiliary, such as a sulfinyl group, is the stability of its conformation. The high stereocontrol achieved using β-ketosulfoxides was due to a chelation effect.[16] For α-phosphoryl-unsaturated sulfoxides the spatial location of the sulfinyl group is forced by a dipole–dipole interaction, where both polar sulfinyl and phosphoryl groups adopt an *anti* orientation. Additional stabilization of the conformations is due to the intramolecular hydrogen bonding between the sulfinyl oxygen atom and the vinyl hydrogen atom.[11c]

Assuming the planar configuration on ylidic carbon atom as proposed earlier for sulfonium ylides[17] we can consider conformations **A** or **B** for ylide **1a** (Fig. 1). Conformer **B** should be strongly favored, since **A** suffers from non-bonded steric interactions between the methyl group on the sulfonium sulfur atom and the aryl sulfinyl substituent. Additionally, conformation **B** can be stabilized by a dipole–dipole interaction (sulfinyl group and ylidic carbon-sulfonium sulfur atom).

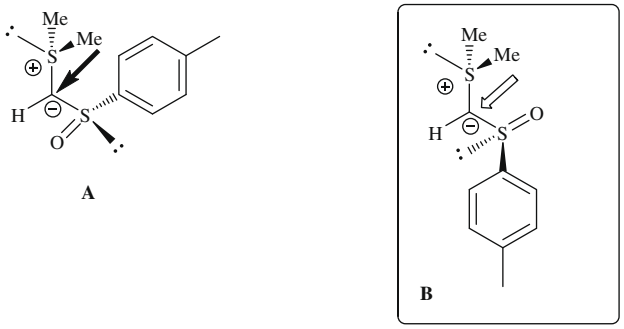

Figure 1. Possible conformers of ylide **1**—rationale for selectivity.

3. Calculations

To gain a better understanding of the factors controlling the stereoselectivity of the cyclopropanation reactions of 1-phosphorylvinyl sulfoxides **1**, density functional theory (DFT) calculations were performed.

Table 1
Epoxidation of aldehydes using ylide **1a**

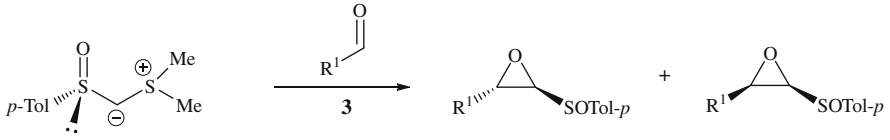

(*S*)-**1a** (2*S*,3*S*,S_S)-**4** (2*S*,3*R*,S_S)-**4**

Entry	Aldehyde	R^1	Method[a]	(2*S*,3*S*,S_S) (%)	2*S*,3*R*,S_S (%)	2*R*,3*R*,S_S (%)	Yield[b] (%)
1	**3a**	Ph	A	60	40	—	69
2	**3a**	Ph	B	71	29	—	70
3	**3a**	Ph	C	68	26	6	56
4	**3a**	Ph	D	80.5	14.0	5.5	78
5	**3a**	Ph	E	72	28	—	67
6	**3b**	*p*-BrC_6H_4	A	59	39.5	1.5	65
7	**3b**	*p*-BrC_6H_4	B	71	27	2	72
8	**3b**	*p*-BrC_6H_4	D	73	21	6	87
9	**3c**	*o*-ClC_6H_4	C	68.5	23	8.5	53
10	**3c**	*o*-ClC_6H_4	D	78.5	19.5	2	86
11	**3d**	*m*-$NO_2C_6H_4$	D	72.5	24	3.5	83
12	**3d**	*m*-$NO_2C_6H_4$	E	64	36	—	68
13	**3d**	2,4-$(NO_2)_2C_6H_3$	C	85.5	14.5	—	74
14	**3e**	2,4-$(NO_2)_2C_6H_3$	D	73.5	20	6.5	76
15	**3f**	α-Nphth	D	91.5	8.5	—	73
16	**3f**	α-Nphth	E	84	12	4	64
17	**3g**	C_4H_9	C	55	45	—	43
18	**3h**	C_5H_{11}	B	55	45	—	76
19	**3i**	C_9H_{19}	A	46	54	—	64
20	**3i**	C_9H_{19}	B	52	48	—	70

[a] Reaction conditions (A) NaH/DMSO, rt. (B) NaH/MeCN, rt. (C) BuLi/THF, 0 °C–rt. (D) K_2CO_3/CH_2Cl_2, rt. (E) KOH/CH_2Cl_2, rt.
[b] Yield of purified two major diastereomers.

Ylides MeS(O)CHSMe$_2$ **1b** and PhS(O)CHSMe$_2$ **1c** and aldehydes MeCHO and PhCHO were used as model compounds for the epoxidation reaction. Detailed calculations were performed for the MeS(O)CHSMe$_2$ + MeCHO reaction. Calculations of the PhS(O)CHSMe$_2$ + PhCHO reaction were carried out to examine the steric effect of larger phenyl groups but only for the limited number of structures, because of the high computational cost.

Calculations indicate that the starting ylides are not planar which implies the diastereomerism of the reactant. They appear in a pyramidal form with the ylide carbon having a configuration close to sp^3 with the C-ylide and S-sulfoxide lone pairs in *gauche* position [for MeS-ylide **1b** the dihedral angle between S–C–S plane and a C–H bond is 128° in the (S_S,*S*)-isomer and 136° in the (S_S,*R*)-isomer]. The Gibbs free energy of the (1*S*,S_S)-diastereomer is about 1.0 kcal/mol lower than that of the (1*R*,S_S)-diastereomer, and the inversion free energy barrier in the gas phase is ca. 3.9 kcal/mol. For PhS-ylide **1c** the Gibbs free energy difference is 0.3 kcal/mol in favour of the (1*S*,S_S)-diastereomer, while the inversion barrier is $\Delta G^{\ddagger}$ = 5.1 kcal/mol. The relatively low inversion barriers indicate that a rapid inversion may take place in solution. Small differences in the free energies of opposite configurations suggest that both enantiomeric forms are represented in significant amounts. Thus, it does not appear to be a factor determining stereochemistry. Pyramidality may be explained by electronic effects: (i) hypeconjugation $p_C \rightarrow \sigma^*_{S-O}$, which is more efficient in sp^3 than in sp^2 configuration on a C atom and (ii) reduction of the C–O lone pair repulsion.[18]

For the above reasons, we considered different conformers of ylide **1** to rationalize the selectivity (Fig. 2).

Figure 2. Stable conformers of ylide **1c** (1*S*,S_S) according to DFT calculations.

Taking this into account, we have calculated four diastereomeric pathways regarding both *transoid* and *cisoid* modes, of the reaction of acetaldehyde with MeS-ylide **1b** which lead to the (2*S*,3*S*,S_S) *and* (2*S*,3*R*,S_S) (Scheme 1), (2*R*,3*R*,S_S) and (2*R*,3*S*,S_S) (Scheme 2) configurations of the epoxides **6**, respectively.

In the gas phase, the most favourable is the *gauche* or *cisoid* approach (in terms of dihedral angle Me$_2$S–C–C=O), as it has a slightly lower (1.4–5.8 kcal/mol) free energy barrier (i.e., lower Gibbs free energy of the transition state) than the *transoid* approach in the diastereomeric pathways shown in Schemes 1 and 2. The *gauche (cisoid)* approach leads to the *cisoid* betaine **5**, which may reversibly dissociate to the substrates or rotate around the C–C bond to a *trans* conformation and subsequently undergo cyclization. We were unable to locate any transition state for the cyclization in the gas phase, since geometry optimisation always led to dissociation of Me$_2$S. Therefore we assumed that the cyclization occurs spontaneously (without energy barrier) once the *transoid* arrangement is achieved.

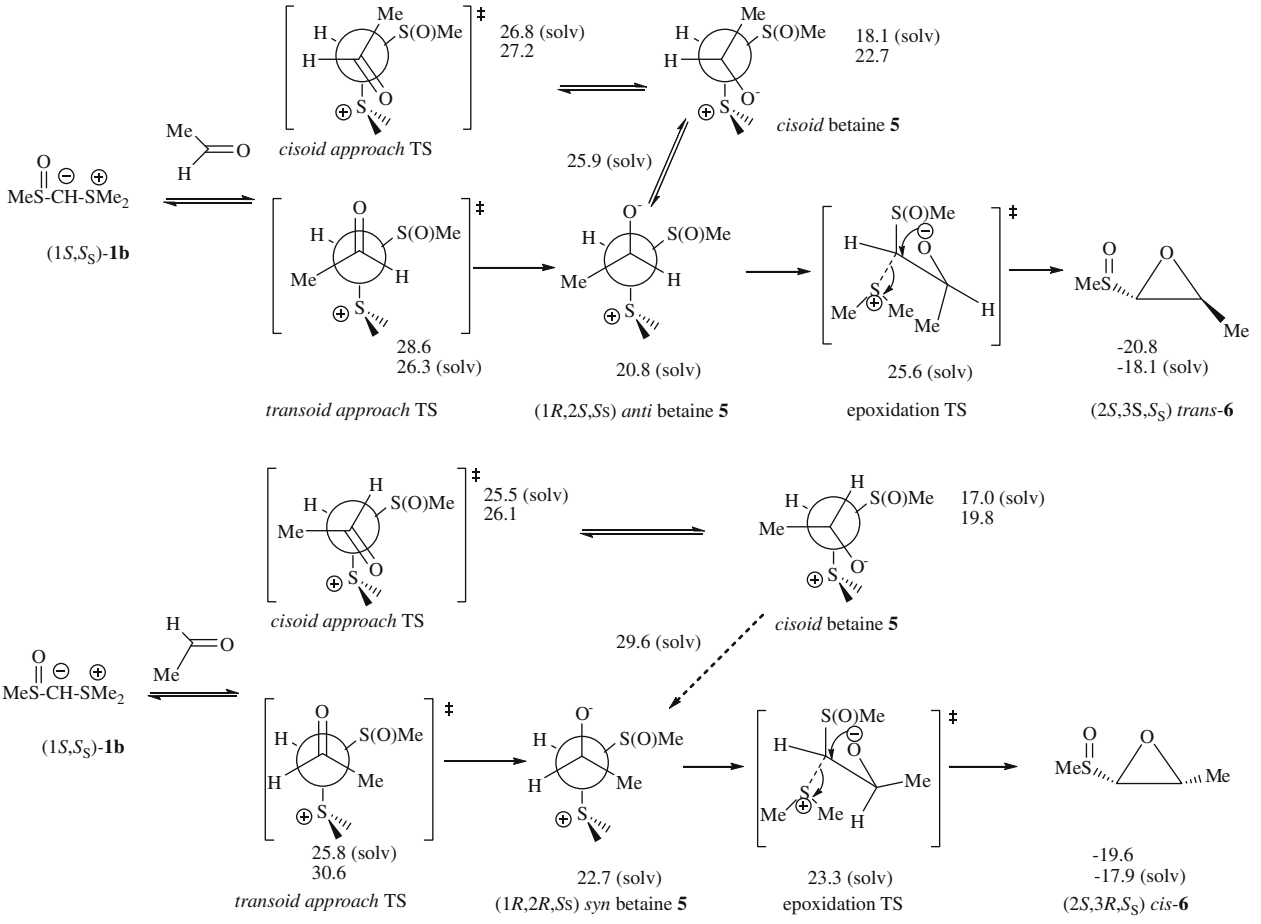

Scheme 1. Diastereomeric pathways of the reaction of acetaldehyde with MeS-ylide **1b** leading to epoxide (2*S*,3*S*,S_S)-**6** and (2*S*,3*R*,S_S)-**6;** numbers shown at structures are the corresponding relative Gibbs free energies in kcal/mol.

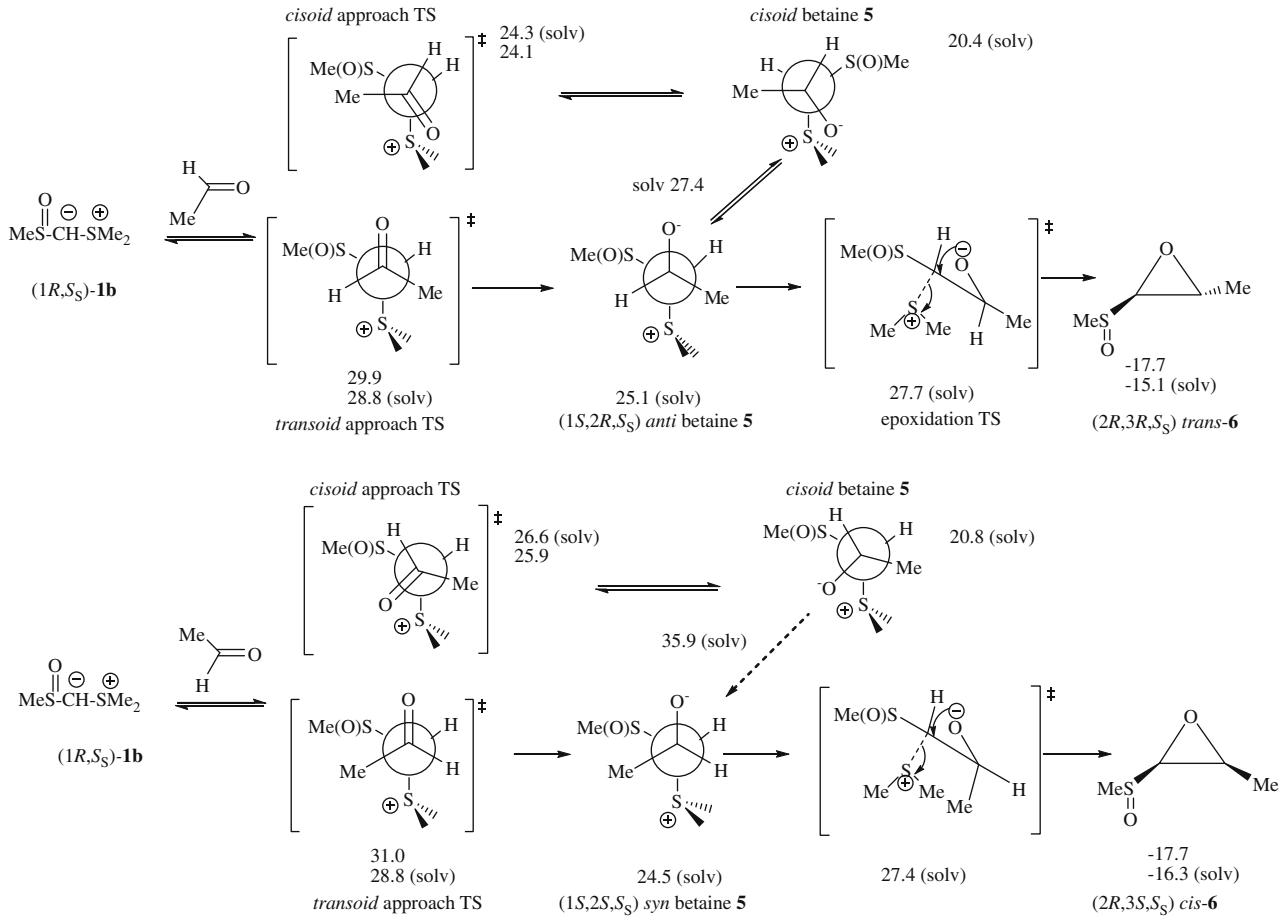

Scheme 2. Diastereomeric pathways of the reaction of acetaldehyde with MeS-ylide **1b** leading to epoxide (2*R*,3*R*,S_S)-**6** and (2*R*,3*S*,S_S)-**6** numbers shown at structures are the corresponding relative Gibbs free energies in kcal/mol.

In the acetonitrile solution, the solvation effect compensates the energy differences and similar values regarding the free energy barriers of *cisoid* and *transoid* approach transition states were obtained where (1*R*,2*S*,S_S) and (1*R*,2*R*,S_S) *transoid* transition states (Scheme 1) are more stable than (1*S*,2*R*,S_S) and (1*S*,2*S*,S_S) *transoid* transition states (Scheme 2) by about 2–3 kcal/mol. Moreover, the SCRF calculations revealed additional transition states leading to cyclization as well as the intermediates resulting from a *transoid* approach (betaines **5**). We can therefore conclude that solvation stabilizes the intermediates in the reaction. Indeed, the charge in the betaines is separated to a greater extent than in the transition states leading to cyclization and therefore better stabilized by polar acetonitrile. As a consequence, elimination of dimethylsulfide now requires passing through a ΔG barrier of 0.7–4.8 kcal/mol relative to the betaine intermediates (Schemes 1 and 2).

Elimination occurs from the *transoid* betaines, in which the O–C–C–S dihedral angle is near 180° which is consistent with the stereochemical course of the S_N2 substitution involving the back-attack of a nucleophile. To reach this rotamer starting from the *cisoid* betaines, it is necessary to pass over a torsional rotational barrier as was postulated by Aggarwal.[19] To examine whether the rotation from *cis*- to *trans*-conformation is possible without dissociation of the C–C bond, we performed a relaxed potential energy scan changing the (Me_2S–C–C–O) angle θ from −180 to 180° for all diastereomers in MeCN searching the structures of stationary points. We found a number of complex rotamers (energy minima) as well as rotational and dissociation–formation transition states. There is a considerable number of stationary points hence we are uncertain whether we have found all of them. The dependence of the relative enthalpy as a function of the θ angle is presented in Figures 3–6.

Figure 3 shows that rotation around the C–C bond without dissociation in the reaction pathway leading to (1*R*,2*S*,S_S)-betaine is possible. For (1*R*,2*R*,S_S)-betaine a rotation is possible only in one

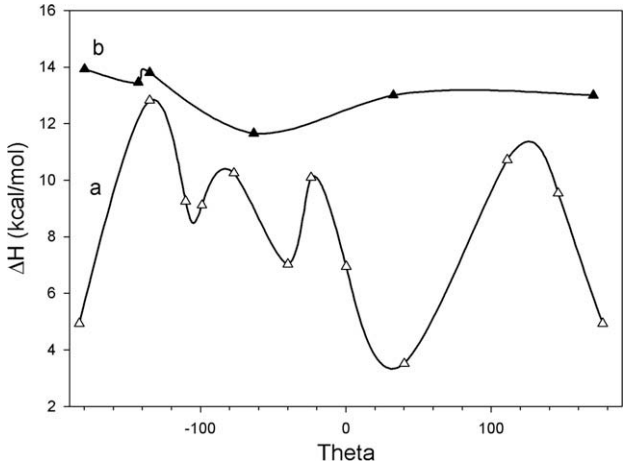

Figure 3. (a) Relative enthalpy profile in MeCN as a function of the dihedral Me_2S–C–C=O angle (rotation around C–C) in the MeS-ylide **1b**-MeCHO (1*R*,2*S*,S_S)-betaine [maxima on enthalpy curve corresponds to rotational transition states]; (b) relative enthalpy profile as a function of dihedral Me_2S–C–C=O angle in dissociation–complexation transition states MeS-ylide + MeCHO (1*R*,2*S*,S_S)-betaine configuration, see Scheme 1. Points are calculated, spline curves are for eye-drawing only.

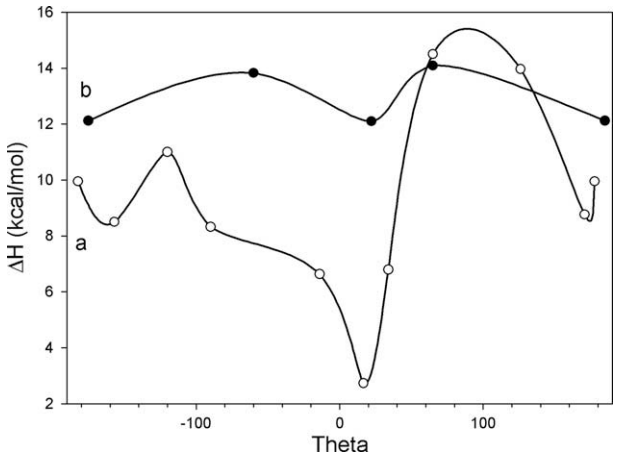

Figure 4. (a) Relative enthalpy profile in MeCN as a function of dihedral Me_2S–C–C=O angle (rotation around C–C) in the MeS-ylide–MeCHO (1*R*,2*R*,S_S)-betaine (maxima on enthalpy curve corresponds to rotational transition states); (b) relative enthalpy profile as a function of dihedral Me_2S–C–C=O angle in dissociation–complexation transition states MeS-ylide + MeCHO (1*R*,2*R*,S_S)-betaine configuration see Scheme 1. Points are calculated, spline curves are for eye-drawing only.

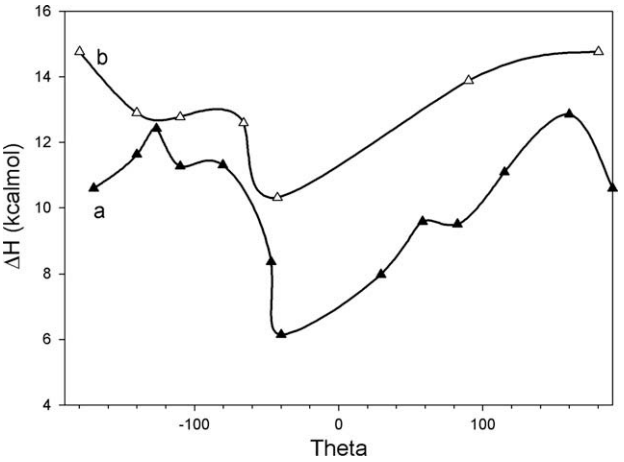

Figure 5. (a) Relative enthalpy profile in MeCN as a function of dihedral Me_2S–C–C=O angle (rotation around C–C) in the MeS-ylide **1b**-MeCHO (1*S*,2*R*,S_S) betaine (maxima on enthalpy curve corresponds to rotational transition states); (b) relative enthalpy profile as a function of dihedral Me_2S–C–C=O angle in dissociation–complexation transition states ylide **1b** + MeCHO (1*S*,2*R*,S_S)-betaine configuration see Scheme 2. Points are calculated, spline curves are for eye-drawing only.

direction. At $\theta \approx 60^\circ$ dissociation of the C–C bond occurs (Fig. 4). Analogous plots for (1*S*,2*R*,S_S)- and (1*S*,2*S*,S_S)-stereoisomers are shown in Figures 5 and 6. In the pathway leading to (1*S*,2*S*,S_S), rotation in both direction results in dissociation (Fig. 6). Interestingly, all betaines are higher in energy than the isolated substrates.

Thermodynamically, epoxidation in all cases is favourable (has negative enthalpy and Gibbs free energy). The stability order of epoxides is as follows: *trans*-(2*S*,3*S*,S_S) > *cis*-(2*S*,3*R*,S_S) > *trans*-(2*R*,3*R*,S_S) > *cis*-(2*R*,3*S*,S_S). In our opinion, it is difficult to distinguish between the cyclization occurring by *cisoid* addition and rotation around the C–C bond to *transoid* position according to the Aggarval concept from reversible addition–dissociation at random positions with cyclization following the *transoid* addition since the free energy barriers corresponding to both reaction mechanisms are very similar.

Calculations for the $PhS(O)CHSMe_2$ **1c** + PhCHO model system were limited to the most important stationary points as the calculations were much more time-consuming (Schemes 3 and 4). Moreover, the SCRF geometry optimizations in many cases failed,

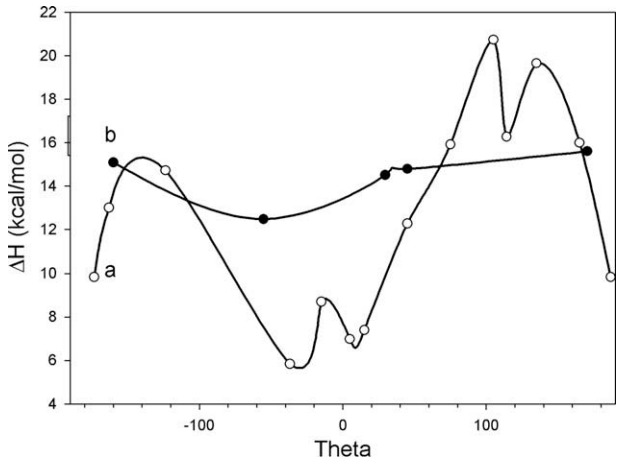

Figure 6. (a) Relative enthalpy profile in MeCN as a function of dihedral Me_2S–C–C=O angle (rotation around C–C) in the MeS-ylide–MeCHO (1*S*,2*S*,S_S) betaine (maxima on enthalpy curve corresponds to rotational transition states); (b) relative enthalpy profile as a function of dihedral Me_2S–C–C=O angle in dissociation–complexation transition states MeS-ylide + MeCHO (1*S*,2*S*,S_S)-betaine configuration see Scheme 2. Points are calculated, spline curves are for eye-drawing only.

and we were not able to find some important stationary points such as rotational transitions states, due to dissociation to the substrates or in some cases to the lack of convergence of the mathematical procedures. Therefore the Gibbs free energies of some structures are only estimated, based on the observation that the SCRF relative free energies in most cases are by 1–1.5 kcal/mol lower than the corresponding free energies in the gas phase.

The general difference between Ph- and Me-substituted model systems is that the free energy barriers for Ph-substituted model system are higher and the thermodynamic exothermic effect upon epoxide formation is smaller. There are also smaller differences between the barriers of the *cisoid* and *transoid* approaches of benzaldehyde. The stability order of epoxides in the gas phase is: *trans*-(2*S*,3*S*,S_S)-**8** > *cis*-(2*S*,3*R*,S_S)-**8** ≈ *trans*-(2*R*,3*S*,S_S)-**8** > *cis*-(2*R*,3*R*,S_S)-**8**. Calculations carried out in the gas phase as well as SCRF calculations showed that the free energy barrier for the reaction pathway leading to *trans*-(2*S*,3*S*,S_S) epoxide is the lowest $\Delta G^{\ddagger}$ = 30.5 kcal/mol (28.4 kcal/mol in acetonitrile), which is in agreement with the observed domination of this diastereomer. The barrier of the reaction pathway leading to *cis*-(2*S*,3*R*,S_S) epoxide ($\Delta G^{\ddagger}$ = 31.1 kcal/mol in acetonitrile) is the same as the barrier of the reaction pathway leading to *trans*-(2*R*,3*R*,S_S) epoxide ($\Delta G^{\ddagger}$ = 31.1 kcal/mol), which suggests that both directions of the reaction are feasible. The least probable seems the formation of the *cis*-(2*R*,3*R*,S_S) epoxide since the barrier is significantly higher ($\Delta G^{\ddagger}$ = 39 kcal/mol).

In the case of the phenyl substituted reagents, the rotation around the C–C bond in betaine is expected to be associated with much higher torsional energy barrier than in the case of methyl derivatives, because of the steric hindrance of the phenyl groups. Inspection of rotation around the C–C bond in the molecular model indicated a large congestion when both phenyl rings are in a *syn*-position; there is also a considerable hindrance between phenyl group in benzaldehyde and the methyl at the sulfonium centre, when the rotation in the opposite direction is assumed (see Fig. 6).Thus, the dissociation–addition mechanism of exchange between *cisoid* and *transoid* approaches is likely to dominate over the rotation around the C–C bond.

4. Discussion

According to the generally accepted mechanism of S-ylide promoted reactions, the key steps consist of the addition of the ylide

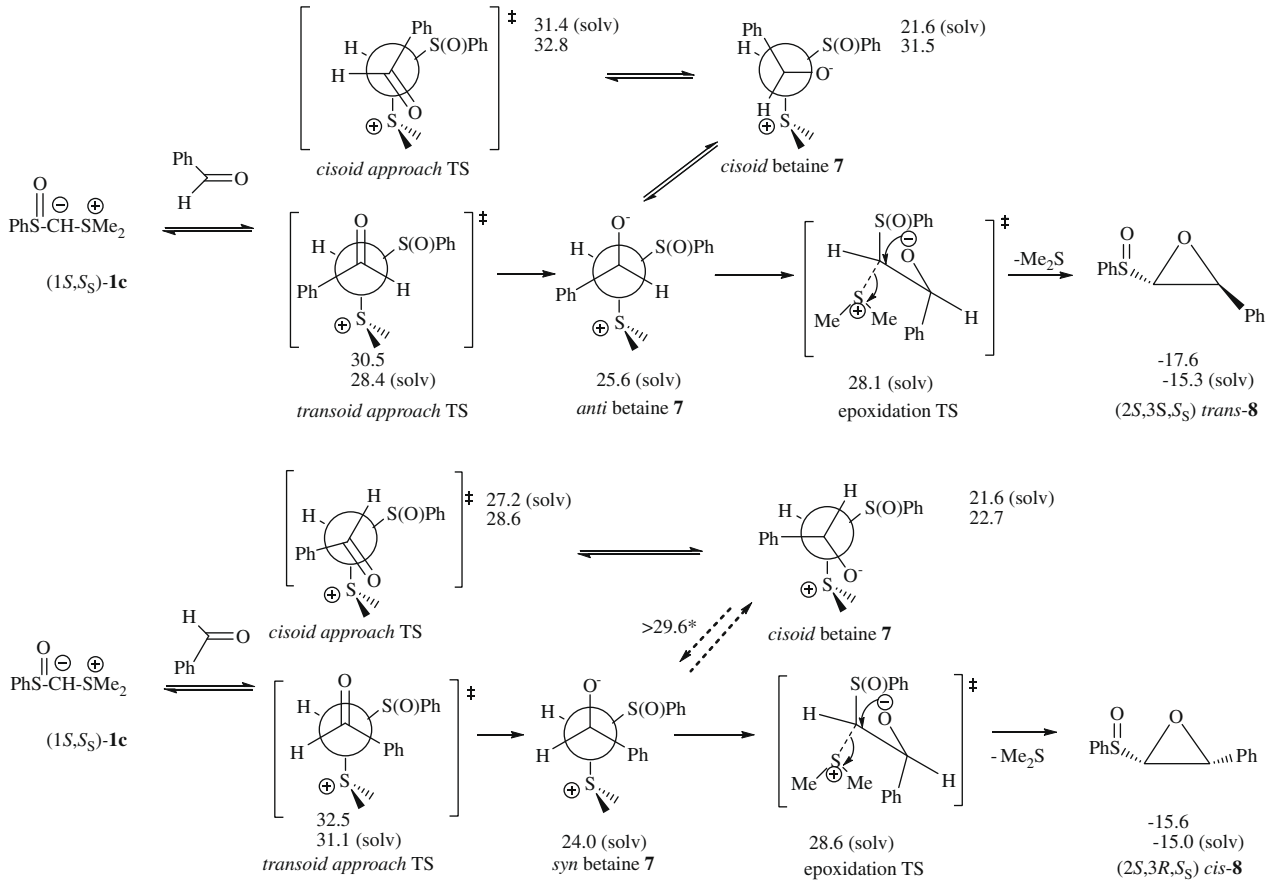

Scheme 3. Gibbs free energies relative to substrates (in kcal/mol) of *cisoid* and *transoid* approach of the reaction of benzaldehyde with PhS-ylide **1c**. * free energy barrier of *cisoid–transoid* transition of (1*R*,2*R*,S_S)-**5;** taking into account a bigger spatial requirement for Ph, this value for (1*R*,2*R*,S_S)-**7** should be much higher.

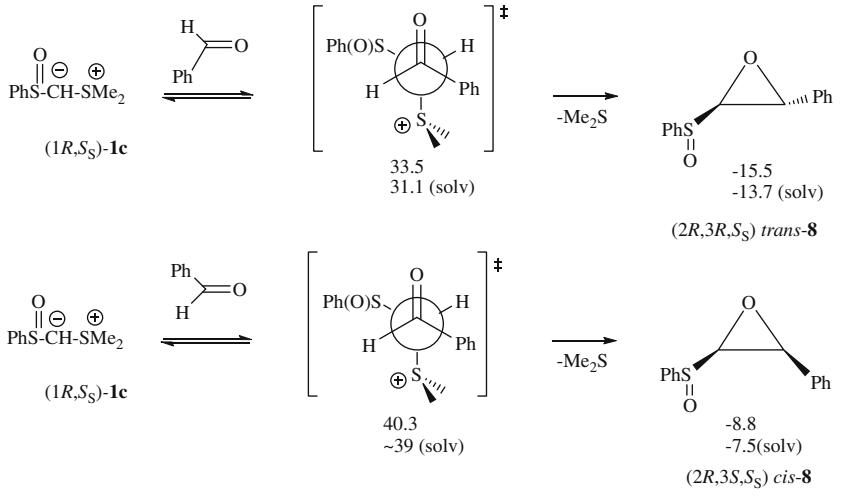

Scheme 4. Gibbs free energies relative to substrates (in kcal/mol)of *transoid* approach of the reaction of benzaldehyde with PhS-ylide **1c**.

to an electrophile to generate a betaine intermediate, rotation around the newly formed C–C bond to achieve the desired antiperiplanar arrangement, and finally the elimination of the sulfur reagent, which generates the three membered ring. The *trans*-epoxide is derived directly from the irreversible formation of the *anti*-betaine. The *cis*-epoxide is derived from the partially reversible formation of the *syn* betaine.

Based on calculations for the model system we tried to explain the stereoselectivity of the epoxidation reaction using (*S*)-dimethylsulfonium-(*p*-tolylsulfinyl)methylide taking into consideration the above mentioned mechanism. Certain differences have arisen from the special structure of the ylide, where the bulky and polar chiral sulfinyl group is bonded to the ylidic carbon atom. The results obtained show that the creation of the *transoid* betaine is

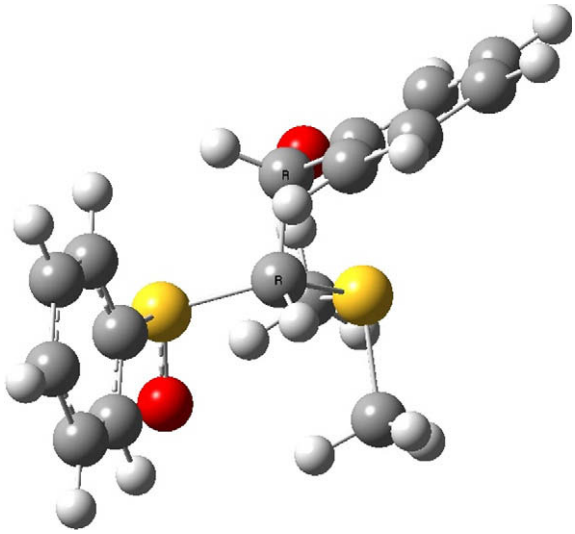

Figure 7. Betaine structure (1*R*,2*R*,S_S) for the addition of PhS(O)CHSMe$_2$ to PhCHO.

the rate-limiting step for all diastereomeric pathways, however it can be achieved in different ways. It has been shown that for this reaction involving highly polar intermediates, analogously to Aggarval's conclusions,[18] continuum solvation models need to be used throughout in order to obtain reasonable results.

In the case of the diastereomeric pathway leading to epoxide *trans*-(2*S*,3*S*,S_S)-**6** there is almost no difference in energy between the *cisoid* and *transoid* approach (Scheme 1), hence both conformers can be formed with the same probability. Moreover, the barrier to torsional rotation is lower compared to the values obtained for other diastereomers, which means that (1*R*,2*S*,S_S)-*anti*-betaine **5** can be achieved quite easily. This betaine is the most stable (ΔG = 20.8 kcal/mol, relative to substrates) of all *transoid* betaines. The barrier of ring closure is smaller than that of dissociation.

The energy required for the *cisoid* approach to achieve (1*R*,2*R*,S_S)-*syn* betaine **5** (Scheme 1) is even smaller than in the former case, but only the *transoid* approach seems to be effective. It was found that the highest activation barrier along this reaction pathway was for the torsional rotation step, from the *gauche* to the *trans* conformation of the betaine. *syn* Betaine **5** is less stable but the low free energy barrier of ring closure (0.6 kcal/mol) allows for easy conversion to epoxide *cis*-(2*S*,3*R*,S_S)-**6.** This explains the lack of *E*/*Z* selectivity for aliphatic aldehydes (Table 1, entries 17–20).

Although these free energy differences are not large, one could expect that upon going to the more bulky substituents, these differences will increase and consequently the ratio of products will change. This prediction corresponds well to the experimental observations for the more bulky systems, where epoxides **4e** and **4f** are formed with the *E*/*Z* ratio being higher than 4–1.

The second *trans*-isomer epoxide (2*R*,3*R*,S_S)-**6** was formed in a very low quantity (under certain reaction conditions this product was not detected at all), which is probably related to the reversibility of this reaction. The highest energy barrier in this case, is attributed to the ring closure step, (Scheme 2) while the less stabilized *transoid* betaine preferentially undergoes the reverse dissociation to substrates. The activation barrier to the ring closure is higher than reversion to the starting materials (relative rates: $k2$ $k-1$).

The free energy of the (1*R*,2*S*,S_S)-transition state [for (2*R*,3*S*,S_S)-*cis*-**6**]is higher by 2.5–3.0 kcal/mol than that of the others, this direction is expected to be disfavoured.

The results for the phenyl-substituted model compared to the methyl-substituted one show close analogies. However, the difference might be that the steric factor associated with the phenyl groups prevents rotation around the C–C bond in the complex, hence the addition–dissociation mechanism seems more likely in this case. Unfortunately, we failed to obtain conclusive data from calculations and this idea is based on qualitative molecular modelling (see Fig. 7).

The high facial stereoselectivity observed in all cases can be attributed to the differences of free energy of betaine formation. It seems to be a consequence of the steric hindrance occurring in the corresponding TS structures. Additionally also the ring closure free energy barrier could also have some influence on the stereochemical outcome of epoxidation since their values of (2*S*,3*S*,S_S)-**6** and (2*S*,3*R*,S_S)-**6** are lower than (2*R*,3*R*,S_S)-**6** and (2*R*,3*S*,S_S)-**6.** The steric factor is also responsible for this difference (Fig. 9).

The *E*/*Z* stereoselection depends on the dimension of the aldehyde substituent and the differences of free energies are manifested for a model reaction using ylide **1c**.

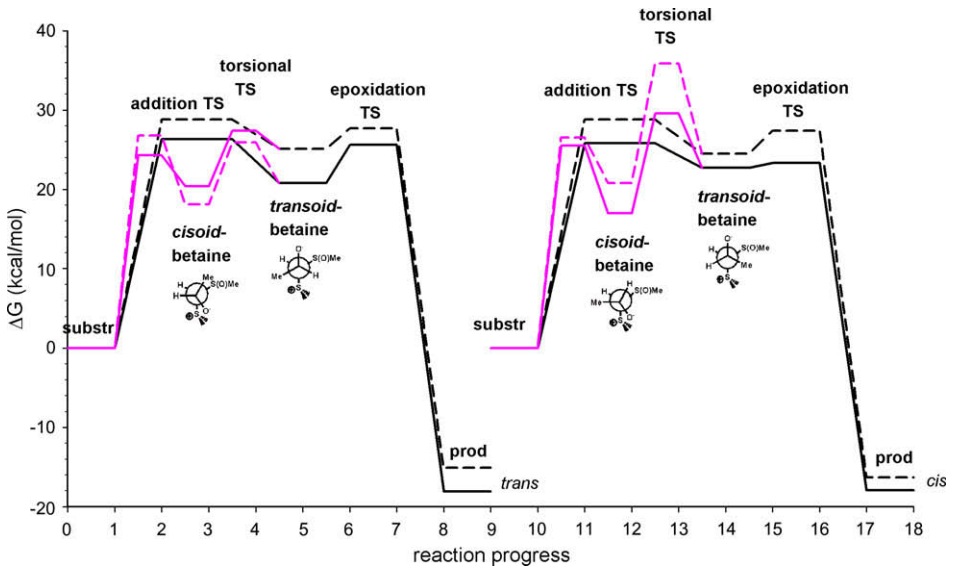

Figure 8. Computed potential enthalpy profile for the model epoxidation reaction in acetonitrile. B3LYP calculated enthalpies of intermediates and transition states are given in kcal/mol. Purple and black curves correspond to *cisoid* and *transoid* addition of acetaldehyde, respectively (see Schemes 1 and 2).

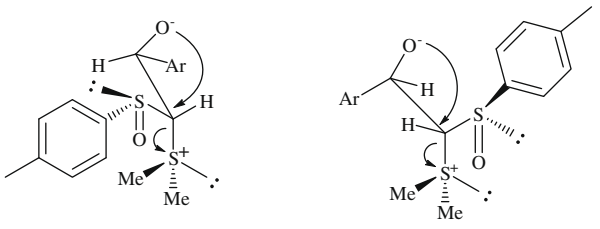

(2*S*,3*S*,S_S)-**5** (2*R*,3*R*,S_S)-**5**

Figure 9. Transition states of ring closure of *transoid* betaines.

Our investigations suggest a big influence caused by the sulfinyl substituent on the sulfonium ylide properties and the mechanism of the epoxidations. First, the non-planar configuration of ylidic carbon atom was established, although energy differences between diastereomers of ylide are very small. Furthermore the barriers of inversion are small, which suggests fast interconversion in solution. From a kinetic point of view of kinetics the epoxidation reaction with sulfinylmethylide is a two-step process, when occurring via *transoid* approach and three-step one assuming a *cisoid* approach followed by rotation around a C–C bond. According to calculations, all four reaction pathways in MeCN solution are probable since differences between energy barriers are relatively small (<5 kcal/mol). However the routes leading to more stable products (*transoid* approaches in Scheme 1, continuous black lines in Fig. 8) seem to be favoured since the overall energy barriers (i.e., the energies of the highest points along the reaction coordinate) are lower than those for routes shown in Scheme 2.

Considering the mechanism of the process, in the case of the pathways leading to both *trans* (2*S*,3*S*,S_S)-**6** and (1*R*,2*R*,S_S)-**6** epoxides (Schemes 1 and 2), the *transoid* approach as well as the *cisoid* approach involving subsequent rotation (proposed by Aggarval) have very similar energy barriers (Fig. 8) and are equally probable. In all the other cases presented in Schemes 1 and 2, the overall energy barriers for the *cisoid* approach/rotation are higher than the *transoid* routes. It is difficult to exclude the *cisoid* approach in the pathway shown in Scheme 1 on the basis of the calculations, because of the small energy differences between the pathways. This is reasonable since the steric hindrance provided by Me groups upon rotation is small. It should be much larger in the case of phenyl substituents and in this case *transoid* approach is expected to be favourable in formation of epoxides. Unfortunately, calculations were too expensive to perform a full conformational search. In particular, optimizations of rotational transition states failed hence we do not know the energy barriers of rotation from *cisoid* to *transoid* conformations for the Ph model. However, it is reasonable to assume that these barriers should be considerably higher than the corresponding barriers for the Me model. Thus the mechanism involving *transoid* approach seems more likely in the case of steric substituents.

5. Experimental

5.1. General

^{1}H, ^{13}C and ^{31}P NMR spectra were recorded on a Bruker MSL 300 and Bruker AC 200 Spectrometer, using deuterochloroform as solvent. Mass spectra were recorded on Finnigan MAT95. IR spectra were recorded on Ati Mattson FTIR Spectrometer. The optical rotations were measured on a Perkin–Elmer 241 MC photopolarimeter in acetone solution. The microanalyses were performed on Elemental Analyzer EA 1108. TLC was carried out on silica gel plates (Merck F254) and Silica Gel 60 (70–230 ASTM) was used for chromatography. THF was freshly distilled over potassium/benzophenone.

5.2. Procedure for preparation of sulfonium salt 2

To 3 mmol (0.6 g) of (−)-(*S*)-*p*-tolyl methylthiomethyl sulfoxide, an excess of MeI (0.5 mL) was added under an argon atmosphere and the mixture was cooled to 0 °C. Next, 0.65 g of $AgBF_4$ was added in small portions and with vigorous stirring. Temperature was maintained for 0.5 h, 5 mL of ethyl ether was added and stirring was continued at rt overnight. After evaporation of ethyl ether the residue was treated with 20 mL of water/acetone mixture (1/1) and filtrated. Then acetone was evaporated, water solution was extracted with 2 × 3 mL of $CHCl_3$ to remove impurities and water was evaporated affording 9 g of crystalline salt **2**: mp 114–116 °C $[\alpha]_D^{22} = -285.9$ (*c* 1.2, acetone); ^{1}H NMR (200 MHz, CD_3COCD_3) δ: 2.43 (3H, s, C*H*$_3$S); 3.05 (3H, s, C*H*$_3$C$_6$H$_4$S); 3.16 (3H, s, C*H*$_3$S); 4.83 and 5.10 (2H, AB system, J = 13.2 Hz, SC*H*$_2$S); 7.49 and 7.73 (4H, AB system J = 8.4 Hz, Ar); ^{13}C NMR (50 MHz) δ: 22.0; 27.3: 27.5; 64.0; 126.0; 131.9; 139.3; 144.9. Anal. Calcd for $C_{10}H_{15}BF_4OS_2$: C, 39.75; H, 5.00. Found: C, 39.64; H, 4.96.

5.3. 3-Phenyl-2-(*p*-tolylsulfinyl)-oxirane 4a

Method A. To a solution of 1 mmol (0.3 g) of (*S*)-dimethylsulfonium-(*p*-tolylsulfinyl)methylide in 5 mL of dry DMSO, 0.52 g (1.1 mmol) of NaH was added at rt under an argon atmosphere. The resulting mixture was stirred for 30 min. Then the precipitate was filtered off and 1 mmol (0.11 g) of benzaldehyde in 1 mL of DMSO was added. After stirring at rt for 2 h, the reaction was quenched with aq NH_4Cl solution (20 mL), extracted with hexane (4 × 5 mL) and dried over $MgSO_4$. After filtration, the solvent was evaporated under reduced pressure to afford **4b** in 82% of yield as a mixture of *trans/cis* isomers in a ratio 1.5/1 (DMSO). Separation of the isomers was achieved by chromatography on basic alumina (hexane–acetone, 50:1).

Method B. To a solution of 1 mmol (0.3 g) of (*S*)-dimethylsulfonium-(*p*-tolylsulfinyl)methyl tetrafluoroborate in 4–5 mL of dry MeCN, 0.52 g (1.1 mmol) of NaH was added at rt under an argon atmosphere. The resulting mixture was stirred for 30 min. Then the precipitate was filtered off and 1 mmol (0.11 g) of benzaldehyde in 1 mL of dry MeCN was added. After stirring at rt for 2 h, the reaction was quenched with aq NH_4Cl solution (20 mL), extracted with hexane (4 × 5 mL) and dried over $MgSO_4$. After filtration, the solvent was evaporated under reduced pressure to afford **3b** in 90% of yield as a mixture of *trans/cis* isomers in a 2.5/1 ratio (MeCN). Separation of isomers was achieved by chromatography on basic alumina (hexane–acetone, 50:1).

Method C. To a suspension of 0.5 mmol (0.15 g) of (*S*)-dimethylsulfonium-(*p*-tolylsulfinyl) methyl tetrafluoroborate in 15 mL of dry THF, 2.75 mL (0.55 mmol) of BuLi was added at 0 °C. The mixture was stirred at this temperature for 1 h and 0.5 mmol (0.055 g) of benzaldehyde in 1 mL of dry THF was added.

Method D. In the round bottom flask equipped with magnetic stirrer 1 mmol (0.3 g) of (*S*)-dimethyl sulfonium-(*p*-tolylsulfinyl)methyl tetrafluoroborate, 1 mmol (0.11 g) of benzaldehyde and 0.2 g of K_2CO_3 was placed. 10 mL of CH_2Cl_2 was added and the mixture was stirred vigorously overnight. Filtration and evaporation of solvent afforded crude product, which was purified by chromatography.

Method E. The mixture of 1 mmol (0.3 g) of (*S*)-dimethyl sulfonium-(*p*-tolylsulfinyl)methyl tetrafluoroborate, 1 mmol (0.11 g) of benzaldehyde and 0.1 g of KOH in 10 mL of CH_2Cl_2 was stirred vigorously overnight. Filtration and evaporation of solvent afforded crude product, which was purified by chromatography.

5.3.1. (2*S*,3*S*,S_S)-3-Phenyl-2-(*p*-tolylsulfinyl)-oxirane 4a

$[\alpha]_D$ = +62.0 (*c* 0.8, acetone). ^{1}H NMR (200 MHz) δ: 2.40 (3H, s, C*H*$_3$C$_6$H$_4$S); 4.00 (1H, d, J = 1.6 Hz, C*H*Ph); 4.58 (1H, d, J = 1.6 Hz,

C*H*S); 7.16–7.45 (7H, Ar); 7.59 (2H, d, *J* = 8.2 Hz). ^{13}C NMR (50 MHz) δ: 21.4; 54.4; 75.6; 124.4; 125.9; 128.5; 129.0; 130.2; 133.8; 137.1; 142.5. Anal. Calcd for $C_{15}H_{14}O_2S$: C, 69.74; H, 5.46. Found: C, 69.61; H, 5.76

5.3.2. (2*S*,3*R*,*S*$_S$)-3-Phenyl-2-(*p*-tolylsulfinyl)-oxirane 4a

$[\alpha]_D = -198.0$ (*c* 0.5, acetone) mp 136–137 °C; ^{1}H NMR (200 MHz) δ: 2.43 (3H, s, C*H*$_3$C$_6$H$_4$S); 4.08 (1H, d, *J* = 3.4 Hz, C*H*Ph); 4.52 (1H, d, *J* = 3.4 Hz, C*H*S); 7.26–7.45 (7H, Ar); 7.61 (2H, d, *J* = 8.3 Hz). ^{13}C NMR (50 MHz) δ: 21.4; 60.7; 74.9; 124.5; 126.6; 128.5; 129.0; 130.1; 131.9; 138.4; 142.2.

5.4. (*p*-Bromophenyl)-2-(*p*-tolylsulfinyl)-oxirane method A, B, and D

5.4.1. (2*S*,3*S*,*S*$_S$)-3-(*p*-Bromophenyl)-2-(*p*-tolylsulfinyl)-oxirane *trans*-4b

$[\alpha]_D^{22} = +52.1$ (*c* 0.6, acetone); mp 136–137 °C ^{1}H NMR (200 MHz, $CDCl_3$) δ: 2.42 (3H, s, C*H*$_3$C$_6$H$_4$S); 3.94 (1H, d, *J* = 1.6 Hz, C*H*Ph); 4.54 (1H, d, *J* = 1.6 Hz, C*H*S); 7.11 and 7.45 (4H, AB system *J* = 8.4 Hz, Ar); 7.36 and 7.59 (4H, AB system *J* = 8.2 Hz, Ar). ^{13}C NMR (50 MHz) δ: 21.5; 53.8; 75.7; 123.1; 124.6; 127.5; 130.3; 131.9; 133.0; 137.0; 142.7. Anal. Calcd for $C_{15}H_{13}BrO_2S$: C, 53.42; H, 3.89. Found: C, 53.61; H, 3.76.

5.4.2. (2*S*,3*R*,*S*$_S$)-3-(*p*-Bromophenyl)-2-(*p*-tolylsulfinyl)-oxirane *cis*-4b

$[\alpha]_D^{22} = -117.1$ (*c* 0.4, acetone); ^{1}H NMR (200 MHz, $CDCl_3$) δ: 2.45 (3H, s, C*H*$_3$C$_6$H$_4$S); 4.08 (1H, d, *J* = 3.3 Hz, C*H*Ph); 4.4 (1H, d, *J* = 3.3 Hz, C*H*S); 7.35 and 7.59 (4H, AB system *J* = 8.4 Hz, Ar); 7.39 and 7.62 (4H, AB system *J* = 8.2 Hz, Ar).

5.4.3. Partial data for 2*R*,3*R*,*S*$_S$-3-(*p*-bromophenyl)-2-(*p*-tolylsulfinyl)-oxirane *trans*-4b

^{1}H NMR (200 MHz, $CDCl_3$) δ: 4.04 (1H, d, *J* = 1.6 Hz, C*H*Ar); 4.30 (1H, d, *J* = 1.6 Hz, C*H*S).

5.5. *o*-Chlorophenyl-2-(*p*-tolylsulfinyl)-oxirane—method C and D

5.5.1. (2*S*,3*S*,*S*$_S$)-3-*o*-Chlorophenyl-2-(*p*-tolylsulfinyl)-oxirane *trans*-4c

$[\alpha]_D^{22} = +38.9$ (*c* 0.75, acetone) ^{1}H NMR (200 MHz, $CDCl_3$) δ: 2.42 (3H, s, C*H*$_3$C$_6$H$_4$S); 3.87 (1H, d, *J* = 1.5 Hz, C*H*Ar); 4.92 (1H, d, *J* = 1.5 Hz, C*H*S); 7.19–7.45 (6H, m, Ar); 7.65 (2H, d, *J* = 8.1 Hz, Ar). ^{13}C NMR (50 MHz) δ: 21.4; 54.8; 75.4; 124.7, 127.2; 128.5: 129.2; 129.6; 130.1, 132.1; 141.7. Anal. Calcd for $C_{15}H_{13}ClO_2S$: C, 61.53, H, 4.48. Found: C, 61.61; H, 4.56.

5.5.2. (2*S*,3*R*,*S*$_S$)-3-*o*-Chlorophenyl-2-(*p*-tolylsulfinyl)-oxirane *cis*-4c

^{1}H NMR (200 MHz, $CDCl_3$) δ: 2.44 (3H, s, C*H*$_3$C$_6$H$_4$S); 4.19 (1H, d, *J* = 3.4 Hz, C*H*Ar); 4.65 (1H, d, *J* = 3.4 Hz, C*H*S); 7.11–7.67 (8H, m, Ar).

5.5.3. Partial data for (2*R*,3*R*,*S*$_S$)-3-*o*-chlorophenyl-2-(*p*-tolyl sulfinyl)-oxirane *trans*-4c

^{1}H NMR (200 MHz, $CDCl_3$) δ: 3.95 (1H, d, *J* = 1.5 Hz, C*H*Ar); 4.76 (1H, d, *J* = 1.5 Hz, C*H*S).

5.6. 3-*m*-Nitrophenyl-2-(*p*-tolylsulfinyl)-oxirane—method D and E

5.6.1. (2*S*,3*S*,*S*$_S$)-3-*m*-Nitrophenyl-2-(*p*-tolylsulfinyl)-oxirane *trans*-4d

$[\alpha]_D^{22} = +55.4$ (*c* 0.6, acetone); ^{1}H NMR (200 MHz, $CDCl_3$) δ: 2.43 (3H, s, C*H*$_3$C$_6$H$_4$S); 4.01 (1H, d, *J* = 1.4 Hz, C*H*Ar); 4.68 (1H, d, *J* = 1.4 Hz, C*H*S); 7.38 (2H, 1/2 AB system *J* = 8.1 Hz, Ar); 7.48–7.63 (m, 4H, Ar); 8.15 (br s, 1H, Ar); 8.17 (m, 1H, Ar). ^{13}C NMR (50 MHz) δ: 21.4; 53.1; 75.6; 121.9; 124.1; 124.7; 130.1; 130.6; 132.4; 133.0; 136.5; 142.5;148.5. Anal. Calcd for $C_{15}H_{13}NO_4S$: C, 59.39; H, 4.32. Found: C, 59.61; H, 4.46.

5.6.2. (2*S*,3*R*,*S*$_S$)-3-*m*-Nitrophenyl-2-(*p*-tolylsulfinyl)-oxirane *cis*-4d

$[\alpha]_D^{22} = -39.2$ (*c* 0.6**,** acetone) ^{1}H NMR (200 MHz, $CDCl_3$) δ: 2.46 (3H, s, C*H*$_3$C$_6$H$_4$S); 4.17 (1H, d, *J* = 3.4 Hz, C*H*Ar); 4.60 (1H, d, *J* = 3.4 Hz, C*H*S); 7.40–7.76 (5H, m, Ar); 7.82–7.85 (1H, m, Ar); 8.27–8.32 (2H, m, Ar).

5.6.3. Partial data for (2*R*,3*R*,*S*$_S$)-3-*m*-Nitrophenyl-2-(*p*-tolylsulfinyl)-oxirane *trans*-4d

^{1}H NMR (200 MHz, $CDCl_3$) δ: 4.14 (1H, d, *J* = 1.7 Hz, C*H*Ar); 4.48 (1H, d, *J* = 1.7 Hz, C*H*S).

5.7. 3-2,4-Dinitrophenyl-2-(*p*-tolylsulfinyl)-oxirane—method C and D

5.7.1. (2*S*,3*S*,*S*$_S$)-3-2,4-Dinitrophenyl-2-(*p*-tolylsulfinyl)-oxirane *trans*-4e

^{1}H NMR (200 MHz, $CDCl_3$) δ: 2.42 (3H, s, C*H*$_3$C$_6$H$_4$S); 3.99 (1H, d, *J* = 1.4 Hz, C*H*Ar); 5.23 (1H, d, *J* = 1.5 Hz, C*H*S); 7.30–7.82 (4H, m, Ar); 8.57–8.62 (2H, m, Ar); 8.95 (1H, d, *J* = 2.2 Hz, Ar). ^{13}C NMR (50 MHz) δ: 21.4; 62.6; 79.4; 121.4; 124.8; 128.8; 129.8; 130.1; 130.9; 141.5; 144.6; 148.7. Anal. Calcd for $C_{15}H_{12}N_2O_6S$: C, 51.72; H, 3.47. Found: C, 51.61; H, 3.76.

5.7.2. (2*S*,3*S*,*S*$_S$)-3-2,4-Dinitrophenyl-2-(*p*-tolylsulfinyl)-oxirane *cis*-4e

^{1}H NMR (200 MHz, $CDCl_3$) δ: 2.45 (3H, s, C*H*$_3$C$_6$H$_4$S); 4.39 (1H, d, *J* = 3.9 Hz, C*H*Ar); 5.05 (1H, d, *J* = 3.9 Hz, C*H*S); 7.38–8.04 (4H, m, Ar); 8.65–8.69 (2H, m, Ar); 9.14 (1H, d, *J* = 2.2 Hz, Ar).

5.7.3. Partial data for 2*R*,3*R*,*S*$_S$-3-2,4-dinitrophenyl-2-(*p*-tolyl sulfinyl)-oxirane *trans*-4e

^{1}H NMR (200 MHz, $CDCl_3$) δ: 4.24 (1H, d, *J* = 1.3 Hz, C*H*Ar); 5.00 (1H, d, *J* = 1.3 Hz, C*H*S).

5.8. 3-α-Naphthyl-2-(*p*-tolylsulfinyl)-oxirane—method D and E

5.8.1. (2*S*,3*S*,*S*$_S$)-3-α-Naphthyl-2-(*p*-tolylsulfinyl)-oxirane *trans*-4f

$[\alpha]_D^{22} = +52.1$ (*c* 0.6, acetone); ^{1}H NMR (200 MHz, $CDCl_3$) δ: 2.40 (3H, s, C*H*$_3$C$_6$H$_4$S); 4.02 (1H, d, *J* = 1.6 Hz, C*H*Ar); 5.14 (1H, d, *J* = 1.5 Hz, C*H*S); 7.25–7.90 (m, 11H, Ar); ^{13}C NMR (50 MHz) δ: 21.4; 55.8; 75.6; 124.1; 124.7; 127.5; 128.5; 129.4; 130.3; 131.3; 132.0; 132.4; 134.0; 137.0; 141.7. Anal. Calcd for $C_{19}H_{16}O_2S$: C, 74.00; H, 5.23. Found: C, 73.81; H, 5.36.

5.8.2. (2*S*,3*R*,*S*$_S$)-3-α-Naphthyl-2-(*p*-tolylsulfinyl)-oxirane *cis*-4f

$[\alpha]_D^{22} = -211.2$ (*c* 0.4, acetone) ^{1}H NMR (200 MHz, $CDCl_3$) δ: 2.44 (3H, s, C*H*$_3$C$_6$H$_4$S); 4.32 (1H, d, *J* = 3.2 Hz, C*H*Ar); 4.96 (1H, d, *J* = 3.2 Hz, C*H*S); 7.31–7.39 (3H, m, Ar); 7.51–7.67 (5H, m, Ar); 7.91–7.95 (2 H, m, Ar); 8.12–8.16 (1H, m, Ar).

5.9. 3-Butyl-2-(*p*-tolylsulfinyl)-oxirane—method B

5.9.1. (2*S*,3*S*,*S*$_S$)-3-Butyl-2-(*p*-tolylsulfinyl)-oxirane *trans*-4g

$[\alpha]_D^{22} = +103.2$ (*c* 0.75, acetone). ^{1}H NMR (200 MHz) δ: 0.87 (3H, t, *J* = 7.0 Hz, C*H*$_3$CH$_2$); 1.25–1.41 (4H, m); 1.58–1.65 (2H, m) 2.40 (3H, s, C*H*$_3$C$_6$H$_4$S); 3.58 (1H, dt, *J* = 1.8, 5.7 Hz, C*H*CH$_2$); 3.66 (1H, d, *J* = 1.8 Hz, C*H*S); 7.33 and 7.53 (4H, AB system *J* = 8.4 Hz, Ar); ^{13}C NMR (50 MHz) δ: 13.7, 21.5; 22.2, 27.8, 30.2, 56.8; 72.7;

124.5; 130.1; 137.9; 142.2. Anal. Calcd for $C_{13}H_{18}O_2S$: C, 65.51; H, 7.61. Found: C, 65.61; H, 7.76

5.10. 3-Pentyl-2-(*p*-tolylsulfinyl)-oxirane—method B

5.10.1. (2*S*,3*S*,S_S)-3-Pentyl-2-(*p*-tolylsulfinyl)-oxirane *trans*-4h

$[\alpha]_D^{22} = +84.5$ (*c* 1.1, acetone); ^{1}H NMR (200 MHz) δ: 0.85 (3H, t, *J* = 6.8 Hz, C*H*$_3$CH$_2$); 1.21–1.39 (6H, m); 1.55–1.65 (2H, m) 2.42 (3H, s, C*H*$_3$C$_6$H$_4$S); 3.59 (1H, dt, *J* = 1.7, 5.7 Hz, C*H*CH$_2$); 3.67 (1H, d, *J* = 1.7 Hz, C*H*S); 7.35 and 7.56 (4H, AB system *J* = 8.2 Hz, Ar); ^{13}C NMR (50 MHz) δ: 13.9, 21.5; 22.4, 25.3, 30.5, 31.2; 56.8; 72.8; 124.4; 130.0; 137.7; 142.3. Anal. Calcd for $C_{14}H_{20}O_2S$: C, 66.63; H, 7.99. Found: C, 66.61; H, 7.76.

^{1}H NMR (200 MHz) δ: 0.86 (3H, t, *J* = 6.8 Hz, C*H*$_3$CH$_2$); 1.22–1.43 (6H, m); 1.58–1.70 (2H, m) 2.42 (3H, s, C*H*$_3$C$_6$H$_4$S); 3.37 (1H, dt, *J* = 3.4, 5.7 Hz, C*H*CH$_2$); 3.82 (1H, d, *J* = 3.4 Hz, C*H*S); 7.35 and 7.60 (4H, AB system *J* = 8.2 Hz, Ar).

5.11. 3-Nonyl-2-(*p*-tolylsulfinyl)-oxirane—method A and B

5.11.1. (2*S*,3*S*,S_S)-3-Nonyl-2-(*p*-tolylsulfinyl)-oxirane *trans*-4i

$[\alpha]_D^{22} = +66.4$ (*c* 0.5, acetone); ^{1}H NMR (200 MHz) δ: 0.87 (3H, t, *J* = 6.8 Hz, C*H*$_3$CH$_2$); 1.25–1.41 (14H, m); 1.58–1.65 (2H, m) 2.40 (3H, s, C*H*$_3$C$_6$H$_4$S); 3.59(1H, dt, *J* = 1.8, 5.7 Hz, C*H*CH$_2$); 3.68 (1H, d, *J* = 1.8 Hz, C*H*S); 7.33 and 7.53 (4H, AB system *J* = 8.4 Hz, Ar); ^{13}C NMR (50 MHz) δ: 13.9, 21.5; 22.2, 22.4, 25.3, 27.8, 30.2, 30.5, 31.2; 31.4, 56.8; 72.8; 124.4; 130.0; 137.7; 142.3. Anal. Calcd for $C_{18}H_{28}O_2S$: C, 70.08; H, 9.15. Found: C, 70.21; H, 9.16.

5.12. Theoretical methods

All calculations were performed using the density functional theory methods with the GAUSSIAN 03 program.[20] Equilibrium geometries in the gas phase were optimized with the B3LYP/6-31G(d) method. All potential energy minima and transition states were identified by the frequency analysis. Transition states were further verified by the IRC calculations. Final electronic energies for the stationary points were calculated at the B3LYP/6-311+G(2d,p) level for the B3LYP/6-31G(d) geometries (this level of theory is denoted as 1B3LYP/6-311+G(2d,p)//B3LYP/6-31G(d)). Thermal corrections to the enthalpy and entropy at 298.15 K were scaled by 0.98. Geometries and energies in acetonitrile solution were calculated using a continuum solvation model and the SCRF–PCM method[21] as implemented in GAUSSIAN 03 at the B3LYP/6-31+G(d) level of theory. Final electronic energies for the stationary points were calculated at the B3LYP/6-311+G(2d,p) level (SCRF-B3LYP/6-311+G(2d,p)//B3LYP/6-31+G(d)). UAHF atomic radii have been used for cavity definition.

References

1. (a) Carreno, M. C.; Hernandez-Torres, G.; Ribagorda, M. *Chem. Commun.* **2009**, 6129–6144; (b) Urbano, A.; Garcıa Ruano, J. L.; Aleman, J.; Cid, M. B.; Fernandez-Ibanez, M. A.; Maestro, M. C.; Martín, M. R.; Martın-Castro, A. M. In *Organosulfur Chemistry in Asymmetric Synthesis*; Toru, T., Bolm, C., Eds.; Wiley-VCH: Weinheim, 2008; pp 55–159; (c) Fernandez, I.; Khiar, N. In *Organosulfur Chemistry in Asymmetric Synthesis*; Toru, T., Bolm, C., Eds.; Wiley-VCH: Weinheim, 2008; pp 265–290; (d) Volonterio, A.; Zanda, M. In *Organosulfur Chemistry in Asymmetric Synthesis*; Toru, T., Bolm, C., Eds.; Wiley-VCH: Weinheim, 2008; pp 351–374; (e) Balcells, D.; Maseras, F. In *Organosulfur Chemistry in Asymmetric Synthesis*; Toru, T., Bolm, C., Eds.; Wiley-VCH: Weinheim, 2008; pp 399–416; (f) Ferber, B.; Kagan, H. *Adv. Synth. Catal.* **2007**, *349*, 493–507; (g) Nenadjenko, G.; Krasovskiy, A. L.; Balenkova, E. S. *Tetrahedron* **2007**, *63*, 12481–12539; (h) Pellissier, H. *Tetrahedron* **2006**, *62*, 5559–5601; (i) Mikolajczyk, M.; Drabowicz, J.; Kielbasinski, P. *Chiral Sulfur Reagents*; CRC: Boca Raton, New York, NY, 1997.
2. (a) Walker, A. J. *Tetrahedron: Asymmetry* **1992**, *3*, 961–998; (b) Solladie, G.. In *Comprehensive Organic Synthesis*; Trost, B. M., Fleming, I., Eds.; Pergamon: Oxford, 1991; pp 148–170. Chapter 3; (c) Khiar, N.; Fernandez, I.; Alcudia, A.; Alcudia, F.. In *Advances in Sulfur Chemistry*; Rayner, C. M., Ed.; JAI: Stanford, CT, 2000; Vol. 2, p 57. Chapter 3; (d) Rayner, C. M. *Contemp. Org. Synth.* **1994**, *1*, 191–203; (e) Procter, D. *J. Chem. Soc., Perkin Trans. 1* **2001**, 335–354.
3. Solladie, G.; Carreno, M. C. In *Organosulfur Chemistry. Synthetic Aspects*; Page, P. C. B., Ed.; Academic: New York, NY, 1995; pp 1–47. Chapter 1.
4. Some recent papers: (a) Gulea, M.; Kwiatkowska, M.; Łyżwa, P.; Legay, R.; Gaumont, A.-C.; Kiełbasiński, P. *Tetrahedron: Asymmetry* **2009**, *20*, 293–297; (b) Mikolajczyk, M.; Midura, W. H.; Ewas, A. M.; Perlikowska, W.; Mikina, M.; Jankowiak, A. *Phosphorus, Sulfur Silicon* **2008**, *183*, 313–325; (c) Brebion, F.; Goddard, J. P.; Fensterbank, L.; Malacria, M. *Synthesis* **2005**, 2449–2452.
5. (a)*Asymmetric Synthesis*; Solladie, G., Morrison, J. D., Eds.; Academic: New York, NY, 1983; Vol. 2, pp 157–199; (b) Cinquini, M.; Cozzi, F.; Montanari, F. In *Organic Sulfur Chemistry, Theoretical and Experimental Advances*; Bernardi, F., Csizmadia, G., Mangini, A., Eds.; Elsevier: Amsterdam, 1985; (c) Hua, D. H.. In *Advances in Carbanion Chemistry*; Snieckus, V., Ed.; JAI: London, 1992; Vol. 1, pp 249–281; (d) Hua, D. H. *Adv. Heterocycl. Nat. Prod. Synth.* **1996**, *3*, 151–177.
6. Finn, M. G.; Sharpless, K. B.. In *Asymmetric Synthesis*; Morrison, J. D., Ed.; Academic Press: Orlando, FL, 1985; Vol. 5, p 247.
7. (a) Katsuki, T. In *Comprehensive Asymmetric Catalysis II*; Jacobsen, E. N., Pfaltz, A., Yammoto, H., Eds.; Springer: Berlin, 1999; pp 621–648; (b) Jacobsen, E. N.; Wu, M. H. In *Comprehensive Asymmetric Catalysis II*; Jacobsen, E. N., Pfaltz, A., Yammoto, H., Eds.; Springer: Berlin, 1999; pp 649–677; (c) Wang, Z.-X.; Tu, Y.; Frohn, M.; Zhang, J. R.; Shi, Y. *J. Am. Chem. Soc.* **1997**, *119*, 11225; (d) Enders, D.; Zhu, J.; Raabe, G. *Angew. Chem., Int. Ed.* **1996**, *35*, 1725.
8. (a) Li, A.-H.; Dai, L.-X.; Aggarwal, V. K. Asymmetric Ylide Reactions: Epoxidation, Cyclopropanation, Aziridination, Olefination, and Rearrangement *Chem. Rev.* **1997**, *97*, 2341–2372; (b) Aggarwal, V. K.. In *Comprehensive Asymmetric Catalysis*; Jacobsen, E. N., Pfaltz, A., Yamamoto, H., Eds.; Springer: Berlin, 1999; Vol. 2, pp 679–693.
9. (a) Satoh, T.; Taguchi, D.; Kurabayashi, A.; Kanoto, M. *Tetrahedron* **2002**, *58*, 4217; (b) Satoh, T.; Kaneko, Y.; Yamakawa, K. *Tetrahedron Lett.* **1986**, *27*, 2379.
10. (a) Furukawa, N.; Sugihara, Y.; Fujihara, H. *J. Org. Chem.* **1989**, *54*, 4222–4224; (b) Julienne, K.; Metzner, P.; Henyron, V. *J. Chem. Soc., Perkin Trans. 1* **1999**, 731–735; (c) Zanardi, J.; Leriverend, C.; Aubert, D.; Julienne, K.; Metzner, P. *J. Org. Chem.* **2001**, *66*, 5620–5623; (d) Winn, C. L.; Bellanie, B.; Goodman, J. M. *Tetrahedron Lett.* **2002**, *43*, 5427–5430; (e) Li, A.-H.; Dai, L.-X.; Hou, X.-L.; Li, Y.-Z.; Huang, F.-W. *J. Org. Chem.* **1996**, *61*, 489–493; (f) Hayakawa, R.; Shimizu, M. *Synlett* **1999**, 1328–1330; (g) Saito, T.; Akiba, D.; Sakairi, M.; Kanazawa, S. *Tetrahedron Lett.* **2001**, *42*, 57–59.
11. (a) Midura, W. H.; Krysiak, J.; Wieczorek, M. W.; Filipczak, A. D. *Pol. J. Chem.* **2007**, *81*, 211–223; (b) Mikołajczyk, M.; Midura, W. H.; Michedkina, E.; Filipczak, A.; Wieczorek, M. W. *Helv. Chim. Acta* **2005**, *88*, 1769–1775; (c) Midura, W. H.; Krysiak, J. A.; Cypryk, M.; Mikołajczyk, M.; Wieczorek, M. W.; Filipczak, A. D. *Eur. J. Org. Chem.* **2005**, 653–662; (d) Garcia Ruano, J. L.; Fajardo, C.; Martin, M. R.; Midura, W. H.; Mikołajczyk, M. *Tetrahedron: Asymmetry* **2004**, *15*, 2475–2482.
12. Midura, W. H. *Synlett* **2006**, 733–736.
13. Numata, T.; Oae, S. *Bull. Chem. Soc. Jpn.* **1972**, *45*, 2794–2796.
14. Colombo, L.; Gennari, C.; Narisano, E. *Tetrahedron Lett.* **1978**, *40*, 3861–3862.
15. Addition of (*S*)-dimethylsulfonium-(*p*-tolylsulfinyl)methylide to *N*-tosyl imines afforded the corresponding sulfinyl aziridines with full enantio- and diastereoselectivity: Midura, W. H. *Tetrahedron Lett.* **2007**, *48*, 3907–3910.
16. (a) Garcia Ruano, J. L.; Martin Castro, A. M.; Roddguez, J. H. *J. Org. Chem.* **1992**, *57*, 7235–7241; (b) Posner, G. H. *Acc. Chem. Res.* **1987**, *20*, 72–78; (c) Solladie, G.; Greck, C.; Demailly, G.; Solladie-Cavallo, A. *Tetrahedron Lett.* **1982**, *23*, 5047–5051.
17. (a) Eades, R. A.; Gassman, P. G.; Dixon, D. A. *J. Am. Chem. Soc.* **1981**, *103*, 1066–1068; (b) Aggarwal, V. K.; Schade, S.; Taylor, B. *J. Chem. Soc., Perkin Trans. 1* **1997**, 2811–2813.
18. Non-planar configuration at the anionic α-carbon atom was suggested previously based on NMR studies and ab initio calculations of α-sulfinylcarbanion. [Chassaing, G.; Marquett, A.; *Tetrahedron*, **1978**, *34*, 1399; Wolfe, S.; Rauk, A.; Csizmadia, I. G. *J. Am. Chem. Soc.* **1967**, *89*. 5710].
19. (a) Aggarwal, V. K.; Harvey, J. N.; Richardson, J. *J. Am. Chem. Soc.* **2002**, *124*, 5747–5756; (b) Aggarwal, V. K.; Richardson, J. *Chem. Commun.* **2003**, 2644–2651.
20. Frisch, M. J.; Trucks, G. W.; Schlegel, H. B.; Scuseria, G. E.; Robb, M. A.; Cheeseman, J. R.; Montgomery, J. A., Jr.; Vreven, T.; Kudin, K. N.; Burant, J. C.; Millam, J. M.; Iyengar, S. S.; Tomasi, J.; Barone, V.; Mennucci, B.; Cossi, M.; Scalmani, G.; Rega, N.; Petersson, G. A.; Nakatsuji, H.; Hada, M.; Ehara, M.; Toyota, K.; Fukuda, R.; Hasegawa, J.; Ishida, M.; Nakajima, T.; Honda, Y.; Kitao, O.; Nakai, H.; Klene, M.; Li, X.; Knox, J. E.; Hratchian, H. P.; Cross, J. B.; Bakken, V.; Adamo, C.; Jaramillo, J.; Gomperts, R.; Stratmann, R. E.; Yazyev, O.; Austin, A. J.; Cammi, R.; Pomelli, C.; Ochterski, J. W.; Ayala, P. Y.; Morokuma, K.; Voth, G. A.; Salvador, P.; Dannenberg, J. J.; Zakrzewski, V. G.; Dapprich, S.; Daniels, A. D.; Strain, M. C.; Farkas, O.; Malick, D. K.; Rabuck, A. D.; Raghavachari, K.; Foresman, J. B.; Ortiz, J. V.; Cui, Q.; Baboul, A. G.; Clifford, S.; Cioslowski, J.; Stefanov, B. B.; Liu, G.; Liashenko, A.; Piskorz, P.; Komaromi, I.; Martin, R. L.; Fox, D. J.; Keith, T.; Al-Laham, M. A.; Peng, C. Y.; Nanayakkara, A.; Challacombe, M.; Gill, P. M. W.; Johnson, B.; Chen, W.; Wong, M. W.; Gonzalez, C.; Pople, J. A. GAUSSIAN *03, Revision D.01*, Gaussian, Inc.: Wallingford, CT, 2004.
21. Tomasi, J.; Persico, M. *Chem. Rev.* **1994**, *94*, 2027.